phys. stat. sol. (c) **2**, No. 7, 2357–2360 (2005) / **DOI** 10.1002/pssc.200461602

Fabrication and analysis of GaN nanorods grown by MBE*

N. A. Sanford[**, 1], **L. H. Robins**[2], **M. H. Gray**[1], **Y.-S. Kang**[2], **J. E. Van Nostrand**[3], **C. Stutz**[3], **R. Cortez**[3], **A. V. Davydov**[2], **A. Shapiro**[2], **I. Levin**[2], and **A. Roshko**[1]

[1] National Institute of Standards and Technology, Optoelectronics Division 815, 325 Broadway, Boulder, Colorado 80305, USA
[2] National Institute of Standards and Technology, Gaithersburg, Maryland, USA
[3] Air Force Research Laboratory, WPAFB, Ohio, USA

Received 31 July 2004, revised 6 September 2004, accepted 27 January 2005
Published online 17 March 2005

PACS 68.37.Lp, 68.65.–k, 78.55.Cr, 78.60.Hk, 78.67.Bf, 81.15.Hi

GaN nanorods were grown on c-plane sapphire substrates under N-rich conditions by plasma-assisted molecular-beam epitaxy. Scanning electron microsopy revealed densely packed nanorods of hexagonal cross section with diameters ranging from roughly 40 to 100 nm. Atomic force microscopy indicated that the rods protruded 50 to 75 nm above the average height of the surface. Transmission electron microscopy (TEM) showed that the nanorods were approximately 1.4 micrometers in length but an accurate measurement of the rod separation was difficult to assess. Contrary to expectations for GaN grown under N-rich conditions, a high density of basal plane stacking faults were not revealed in TEM under typical imaging conditions. X-ray diffraction using the (0002), (0004), (0006), $(10\bar{1}4)$, and $(10\bar{1}5)$ reflections yielded c = 0.5188 ± 0.0002 nm and a = 0.3188 ± 0.0004 nm. Low temperature photoluminescence and cathodoluminescence showed broad near-bandgap emission around 3.4 eV that shifted to the blue with reduced temperature in the usual manner, and the presence of a similarly blue-shifting peak near 3.2 eV. The spectra were deconvolved using nine lineshape functions revealing 2 phonon replicas asssociated with the peak near 3.2 eV. Room temperature spectroscopic reflection fited to the standard Aspnes third-derivative lineshape function yielded a transition energy of 3.407 eV for the A exciton and 3.490 eV for the B+C excitons (not spectrally resolved). Both the x-ray and photoreflectance results indicate that the nanorods are fairly relaxed.

1 Introduction

Wide bandgap III-nitride nanorods and nanowires are showing promise as an interesting new low defect density material system with potential applications in optoelectronics and chemical sensors. Many of these emerging applications have been realized using GaN nanowires grown by catalyst methods and examples of nanowire-based lasers, LEDs, and sensors are illustrated in reference [1]. Recently, AlGaN nanorods of exceptionally low defect density have been grown using plasma-assisted molecular beam epitaxy (PAMBE) by Ristić et al. [2]. In the same article, the authors also showed that GaN nanodisks could be incorporated into the nanorods without disrupting the cylindrical growth mode of the structures. A striking observation reported in this work is that high-resolution TEM reveals no discernible defects in the AlGaN nanorod structures or in the nanorods with GaN nanodisks. These recent publications and

[*] Contribution of an agency of the United States government.
[**] Corresponding author: e-mail: sanford@boulder.nist.gov, Phone: +01 303 497 5239, Fax: +01 303 497 3387

results therefore compel further study of GaN nanorods grown via MBE and further research into functional devices that may be realized in such structures.

2 Crystal growth and structural characterization

GaN nanorods were grown by PAMBE on c-plane sapphire substrates 50.8 mm in diameter. Ga and Al were provided by standard Knudsen cells and nitrogen was supplied via an RF plasma source fed by 99.999% purity nitrogen. A 15 nm layer of AlN was first deposited resulting in Ga polar growth of the GaN layer. Growth of GaN nanorods was performed by maintaining the V/III flux ratio >20. This resulted in a spotty RHEED pattern with no 1×1 streaks. SEM images of the columnar growth are illustrated in Fig. 1. AFM scans of the sample (not shown) reveal that some of the rods protrude 50 to 75 nm above the average surface height of the sample. Correspondingly, the nanorod ends appearing white in the plan-view FESEM image also protrude above the surface of the sample.

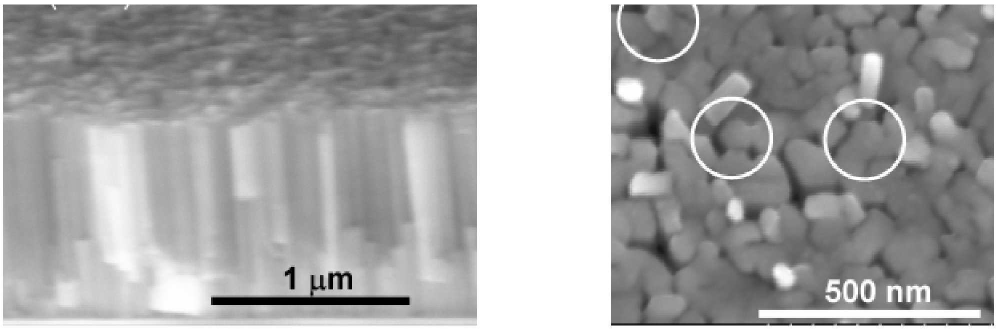

Fig. 1 SEM cross sectional image (left) and FESEM plan-view image (right) of the PAMBE grown nanorod structure. The rods are densely packed but still discernible in the cross-sectional image. The hexagonal cross section of the rods is highlighted by circles in the plan-view image.

X-ray diffraction studies were performed in order to measure the a and c lattice constants for the sample. Scans were taken for the (0002), (0004), (0006), $(10\bar{1}4)$, and $(10\bar{1}5)$ reflections for two different phi orientations separated by 120°. This yielded c = 0.5188 ± 0.0002 nm and a = 0.3188 ± 0.0004 nm. The rocking curve width for (0002) was 0.36° (1296 arcsec) FWHM.

The sample was also examined with cross sectional TEM. These results are summarized in Figs. 2 and 3. The most notable feature of the TEM analysis was that for the beam orientation along the $[2\bar{1}\bar{1}0]$ zone axis, considerable streaking was observed parallel to $[01\bar{1}0]$. Contrary to what would normally be expected for nitrogen rich growth conditions [3, 4], there was an absence of streaks observed parallel to [0001] in these diffraction patterns. These results indicate that there is a low density of basal plane stacking faults in the sample compared to earlier work describing nitrogen rich growth conditions [3, 4]. The results illustrated in Fig. 2 suggest that laminar structures roughly 10 nm in thickness

Fig. 2 TEM diffraction patterns for the beam directed along the $[2\bar{1}\bar{1}0]$ and $[10\bar{1}0]$ zone axes.

and perpendicular to the basal plane are responsible for the streaking. Plan view TEM studies are underway to test this hypothesis. Finally, Fig. 3 illustrates bright field TEM images of the sample in cross section. Once again, clear evidence for basal plane stacking faults is absent from these images.

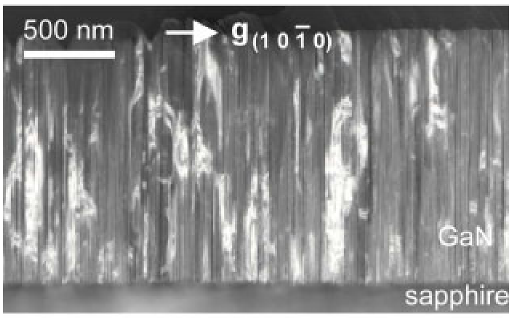

Fig. 3 (a) Bright field image with the diffraction vector **g** as indicated. The nanorod layer is roughly 1400 nm thick.. The separation between the rods is not well resolved.

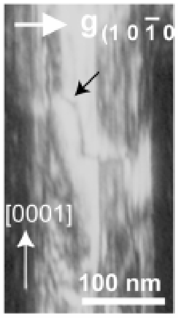

Fig. 3 (b) The defect feature indicated by the black arrow was observed in many of the individual nanorods.

3 Optical characterization

Variable temperature photoluminescence (PL), cathodoluminescence (CL), and room temperature spectroscopic reflection measurements were performed on the sample. PL and CL results are illustrated in Fig. 4. In the PL measurements, spectra were collected at a location roughly 15 mm from the center of the wafer while the sample was pumped with a cw HeCd laser operating at 325 nm. The pump intenstiy on the sample was approximately 60 W/cm^2. The CL spectra were collected at 12 K from several locations ranging from near the center to near the edge of the wafer. The sample was tilted 45° from the incident electron beam and the acceleration voltage was 9.1 kV. Under these conditions, the average electron penetration depth was 135 nm and the maximum electron penetration depth was 397 nm.

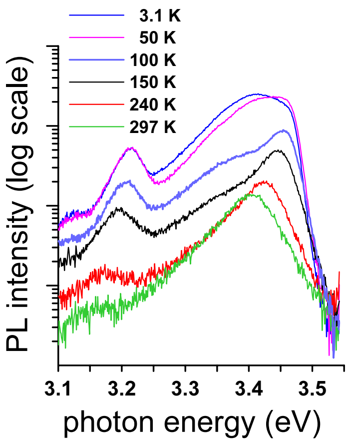

Fig 4 (a) PL recorded at several different temperatures at a location roughly 15 mm from the center of the wafer.

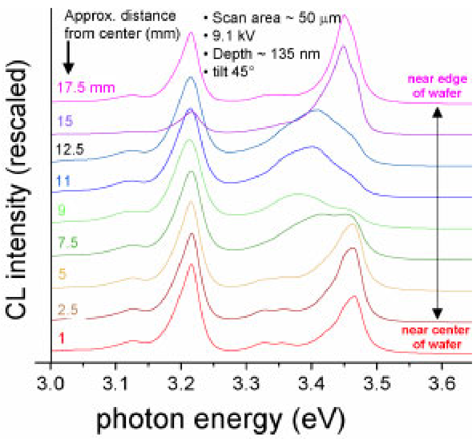

Fig. 4 (b) CL recorded at several different locations between the center ant the edge of the wafer. The sample temperature was 12 K.

Additionally, no substantial defect or "yellow band" luminescence was observed for CL spectra recorded in the range from 1.6 to 3.0 eV. The broad PL and CL spectra were deconvolved with a set of 9 hyperbolic secant lineshape functions. An example of this fitting procedure applied to CL data is shown in Fig. 5. Finally, room temperature photoreflectance measurements were taken at several radial location across the wafer. Fitting of these data to the standard Aspnes third-derivative lineshape function [5] revealed a transition energy of 3.407 eV for the A exciton and 3.490 eV for the B+C excitons (not spectrally resolved).

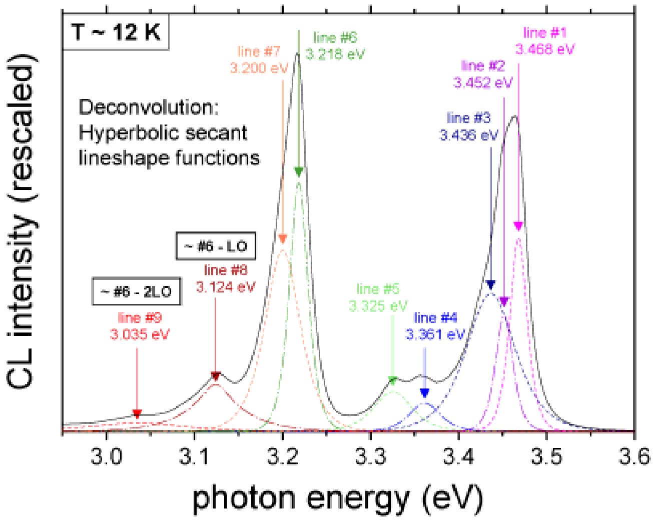

Fig. 5. Deconvolution of CL spectrum collected 2.5 mm from the center of the wafer. The spectrum is fit to 9 hyperbolic secant functions. Lines 8 and 9 fit to the first and second phonon replicas of line 6.

4 Summary and continuing work

The key findings of this work are: (i) The results of both the x-ray analysis and the photoreflectance measurements suggest that the GaN layer is substantially relaxed; (ii) although a 3D growth mode has been achieved, both the SEM and TEM results show that the nanorods are too densely packed to facilitate optical or structural studies of individual rods; (iii) the expected propensity of N-rich growth conditions to produce a high density of basal plane stacking faults was not observed in the present study; (iv) the streaking parallel to $[10\bar{1}0]$ observed in TEM diffraction patterns suggests the presence of laminar defect structures, of roughly 10 nm thickness, that lay perpendicular the the basal plane; (v) in the deconvolved CL spectra, peak #1 likely arises from free or donor-bound exciton transitions while peak #2 likely arises from acceptor bound transitions; (vi) the thermal quenching behavior of peaks #3 through 9 suggest that these transitions may originate from excitons bound to as yet unidentified structural defects; (vii) peaks #6 and 7 near 3.2 eV appear to correlate with similar spectral features observed from MBE-grown Ga or N polar films that have been recently reported [6].

Efforts are ongoing to further quantify the observed streaking in the TEM diffraction patterns for the present samples. Additionally, work aimed at controlling the density of the nanorod growth, through modifications of the MBE growth techniques and the use of nanotemplating methods, is underway.

Acknowledgement Partial support of the work performed at AFRL was provided by Lt. Col. Todd Steiner.

References

[1] J. C. Johnson, et al., Nature Mater. 1, 106 (2002); Y. Huang, et al., Nano Lett. 2, 101 (2002).
[2] J. Ristić, et al., Phys. Rev. B 68, 125305 (2003).
[3] T. Araki, Y. Chiba, and Y. Nanishi, J. Cryst. Growth 210, 162 (2000).
[4] E. J. Tarsa, et al., J. Appl. Phys. 82, 5472 (1997).
[5] D. E.Aspnes, in: Handbook of Semiconductors Vol. 2, edited by M. Balkanski (North Holland, New York, 1980), pp. 109–154.
[6] M. A. Reshchikov et al., J. Appl. Phys. 94, 5623 (2003).